Simultaneous time-lapse full waveform inversion

Musa Maharramov and Biondo Biondi

ABSTRACT

We propose a technique for improving the robustness of time-lapse full waveform inversion by reducing numerical artifacts that contaminate inverted model differences. More specifically, we demonstrate that simultaneously inverting for baseline and monitor models in combination with a Tikhonov regularization applied to the model difference can reduce acquisition-related repeatability issues and spurious numerical artifacts arising in separate baseline and monitor inversions. We demonstrate our method using a synthetic model problem and describe a simplified "cross-updating" approach that can be applied to large-scale time-lapse industrial problems using the existing FWI inversion tools.

INTRODUCTION

Time-lapse full waveform inversion (FWI) (Watanabe et al., 2004; Routh et al., 2012) is a promising technique for time-lapse seismic imaging where production-induced subsurface model changes are within the FWI resolution. However, like alternative time-lapse techniques, time-lapse FWI is sensitive to *repeatability issues* (Asnaashari et al., 2012). Non-repeatable acquisition geometries (e.g., slightly shifted source and receiver positions), acquisition gaps (e.g., due to previously absent obstacles), different source signatures and measurement noise – all contribute to differences in the data from different survey vintages. Differences in the input datasets due to repeatability issues may easily mask out valuable production-induced changes. However, even with the simple noise-free synthetic data in the absence of *acquisition* repeatability issues, numerical artifacts may easily contaminate the inverted difference of monitor and baseline when practical limitations are imposed on solver iteration count. We propose a computationally feasible and robust time-lapse FWI that minimizes model differences outside of areas of production-induced change by simultaneously inverting for multiple models, and imposing a regularization condition on model differences.

THE METHOD

Full waveform inversion is defined as solving the following optimization problem (Virieux and Operto, 2009; Plessix et al., 2010)

$$\|\mathbf{Mu} - \mathbf{d}\| \;\rightarrow\; \min \tag{1}$$

where $\mathbf{M}, \mathbf{d}$ are the measurement operator and data, $\mathbf{u}$ is the solution of a forward-modeling problem

$$\mathbf{D}(\mathbf{m})\mathbf{u} \;=\; \phi, \tag{2}$$

where $\mathbf{D}$ is the forward-modeling operator that depends on a *model* vector $\mathbf{m}$ as a parameter, and ϕ is a source. The minimization problem 1 is solved with respect to both the model $\mathbf{m}$ and source ϕ, or just the model. In the frequency-domain formulation of the acoustic waveform inversion, the forward-modeling equation 2 becomes

$$-\omega^2 u - v^2(x^1, \ldots, x^n)\Delta u \;=\; \phi(\omega, x^1, \ldots, x^n) \tag{3}$$

where ω is a temporal frequency, n is the problem dimension, v is the acoustic wave propagation velocity. Values of the seismic velocity at all the points of the modeling domain constitute the model parameter vector $\mathbf{m}$. Rock density can be incorporated in the problem but we omit it here for simplicity. Direct problem 2 can be solved in the frequency domain, or in the time domain followed by a Fourier transform in time (Virieux et al., 2009). Inverse problem 1 is typically solved using a multiscale approach, from low to high frequencies, supplying the output of each frequency inversion to the next step.

FWI applications in time-lapse problems seek to recover *production-induced* changes in the subsurface model (Barkved and Kristiansen, 2005) using multiple data sets from different acquisition vintages. For two surveys sufficiently separated in time, we call such datasets (and the associated models) *baseline* and *monitor*.

Time-lapse FWI can be carried out by separately inverting the baseline and monitor models (*parallel difference*) or inverting them sequentially with e.g. the baseline supplied as a starting model for the monitor inversion (*sequential difference*). Another alternative is to apply the *double difference* method, with a baseline model inversion followed by a monitor inversion that solves the following optimization problem

$$\| \left(\mathbf{M}^s_m \mathbf{u}_m - \mathbf{M}^s_b \mathbf{u}_b\right) - \left(\mathbf{M}_m \mathbf{d}_m - \mathbf{M}_b \mathbf{d}_b\right) \| \;\rightarrow\; \min \tag{4}$$

by changing the monitor model (Watanabe et al., 2004). The subscripts in equation 4 denote the baseline and monitor surveys, $\mathbf{d}$ denotes the field data, and the $\mathbf{M}$s are measurement operators that project the synthetic and field data onto a common grid, the superscript s denotes the measurement operators applied to the synthetic data. Although the double difference method offers potential advantages for tackling acquisition-related repeatability issues, it was shown to be more sensitive to uncorrelated noise (Asnaashari et al., 2012) in addition to requiring data projection onto a common grid.

In all of the described techniques optimization is carried out with respect to a *single* model, albeit of different vintages at different stages of the inversion. In our method we propose to invert for the baseline and monitor models *simultaneously* by

solving the following optimization problem:

$$\alpha\|\mathbf{M}_b\mathbf{u}_b - \mathbf{d}_b\|^2 + \beta\|\mathbf{M}_m\mathbf{u}_m - \mathbf{d}_m\|^2 + \tag{5}$$

$$\gamma\| \left(\mathbf{M}_m^s\mathbf{u}_m - \mathbf{M}_b^s\mathbf{u}_b\right) - \left(\mathbf{M}_m\mathbf{d}_m - \mathbf{M}_b\mathbf{d}_b\right) \|^2 + \tag{6}$$

$$\|\mathbf{W}_b\mathbf{R}_b(\mathbf{m}_b - \mathbf{m}_b^{\text{PRIOR}})\|^2 + \tag{7}$$

$$\|\mathbf{W}_m\mathbf{R}_m(\mathbf{m}_m - \mathbf{m}_m^{\text{PRIOR}})\|^2 + \tag{8}$$

$$\|\mathbf{WR}(\mathbf{m}_m - \mathbf{m}_b - \Delta\mathbf{m}^{\text{PRIOR}})\|^2 \;\rightarrow\; \min, \tag{9}$$

with respect to both the baseline and monitor models $\mathbf{m}_b$ and $\mathbf{m}_m$. The terms 5 correspond to separate baseline and monitor inversions, the term 6 is the optional double difference term, the terms 7,8 are optional separate baseline and monitor inversion Tikhonov regularization terms (Aster et al., 2012), and the term 9 represents Tikhonov regularization of the model difference. The $\mathbf{R}$ and $\mathbf{W}$ denote regularization and weighting operators respectively, with the subscript denoting the survey vintage where applicable.

A joint inversion approach was proposed earlier in applications to the linearized waveform inversion (Ayeni and Biondi, 2012). In this work, we propose a simultaneous full waveform inversion with special emphasis on the regularization of model difference in equation 9. Constraining the model difference where production-induced changes are expected to be negligible while simultaneously solving for both baseline and monitor models can be expected to reduce both spurious numerical artifacts and non-repeatable acquisition related artifacts in the model difference. The traditional sequential and double difference methods, on the other hand, make artifact reduction less effective by allowing only one model to change.

An implementation of the proposed simultaneous inversion algorithm requires solving a nonlinear optimization problem of twice the data and model dimension of problems 1 and 4. To allow an immediate practical application of the proposed methodology using the existing single-model solvers, we propose a *cross-updating* technique that offers a crude but remarkably effective approximation to minimizing the objective function 5 and 9. This cross-updating technique consists in one standard run of the sequential difference algorithm, followed by a second run with the inverted monitor model supplied as the starting model for the second baseline inversion

$$\mathbf{m}_{\text{INIT}} \rightarrow \text{BASE INV} \rightarrow \text{MON INV} \rightarrow \text{BASE INV} \rightarrow \text{MON INV}, \tag{10}$$

and taking the difference of the latest inverted monitor and baseline models. Process 10 can be considered an approximation to minimizing 5 and 9 because non-repeatable footprints of both inversions are accumulated in both models, canceling out in the difference. In both the full simultaneous inversion and cross-updating methods, we expect the models to be brought closer together wherever either of them cannot be reliable resolved. Note that this process is not guaranteed to improve the results of the individual inversions but is only proposed for improving the model difference.

RESULTS

We demonstrate our proposed simultaneous inversion method and its cross-updating approximation 10 on a one-dimensional model problem. We are trying to recover the difference between the true baseline and monitor models, as respectively shown in Fig 1(b), 1(a). Equation 3 is discretized on the equispaced grid of 32 points spanning the modeling interval $[0, 1]$. We use different baseline and monitor source wavelets (see Fig 2) and use a multiscale inversion from 0.2Hz to 1Hz with a .2Hz step, solving the optimization problems 1 and 5,9 using the hybrid Fletcher-Reeves-Polar-Ribièr method (Nocedal and Wright, 2006). In the first experiment the data is noise-free and receivers are located at every node of the computational grid. In the second experiment we add 5% high-wavenumber noise to the data and allow receiver positions to shift randomly by up to half the grid step. No prior model or model difference was used in the objective function 5,9.

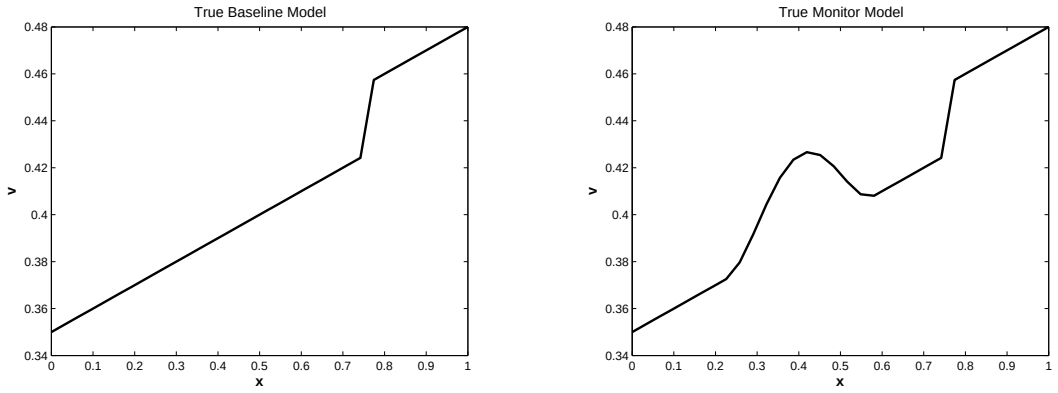

(a) (b)

Figure 1: True baseline and monitor models for 1D simultaneous inversion test. [**CR**]

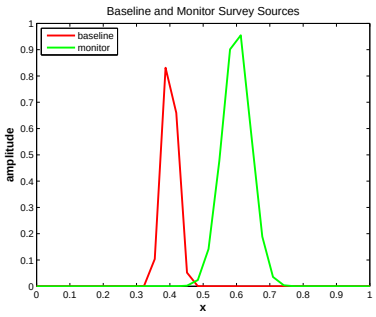

Figure 2: Sources used for generating synthetic baseline and monitor surveys. [**CR**]

To demonstrate that the improvements delivered by the cross-updating procedure 10 are not simply due to the increased number of iterations, we use the following procedure for "iterated" sequential inversion:

$$\begin{aligned} \mathbf{m}_{\text{INIT}} &\rightarrow \text{BASE INV} \rightarrow \text{MON INV} \rightarrow \text{MON INV} \\ \mathbf{m}_{\text{INIT}} &\rightarrow \text{BASE INV} \rightarrow \text{BASE INV}. \end{aligned} \tag{11}$$

Note that process 11 uses the same number of full waveform inversions as 10. We compare method 11 with the cross-updating 10 and the simultaneous inversion by optimizing the objective function 5,9. In our tests, we set the terms 6-8 to zero and use only a model difference regularization. We use Laplacian as the regularization operator **R**, and the weighting operator **W** is a simple mask zeroing out the area of expected model change.

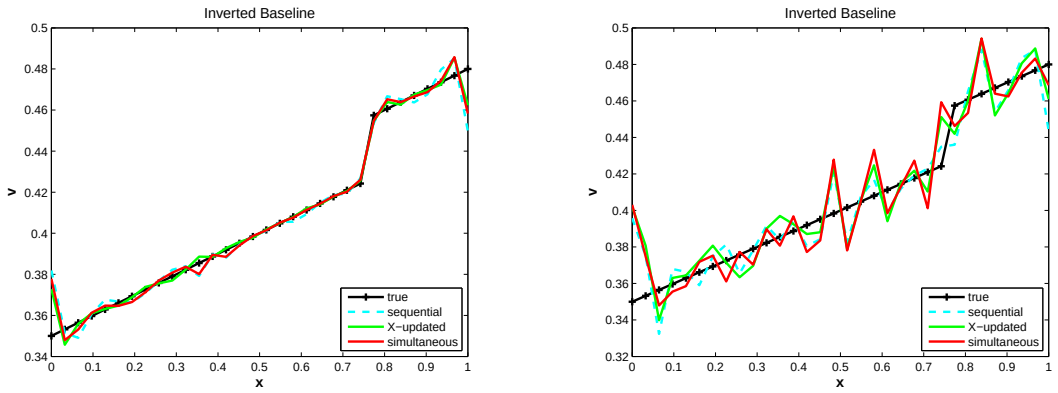

(a) (b)

Figure 3: Inverted baseline: (a) no noise (b) 5% noise and $.5\Delta x$ random receiver mispositioning. [**CR**]

Fig 3(a), 4(a), 5(a) show the results of the three algorithms for the noise-free experiment. Both the simultaneous inversion result and the cross-updating approximation exhibit fewer artifacts outside of the area of production-induced changes than does the sequential approximation. Fig 3(b), 4(b), 5(b), 6(b) show the results of the

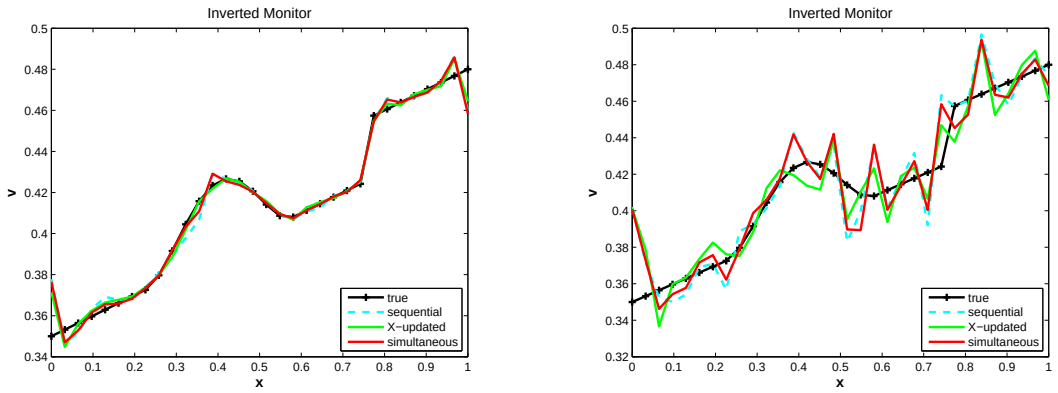

(a) (b)

Figure 4: Inverted monitor: (a) no noise (b) 5% noise and $.5\Delta x$ random receiver mispositioning. [**CR**]

second experiment with added noise and receiver mispositioning. The improvement

achieved by the simultaneous inversion and cross-updating methods is quite dramatic, with the simple cross-updating method still delivering a good qualitative picture of the model difference. One key feature of the plotted models of Fig 3(b), 4(b) is that the inverted models seem to inherit each other's peaks and deviations from the true model even though *different random noise* is added to the baseline and monitor data. This confirms our conjecture that the model-difference regularization will bring the models closer together where either model cannot be reliably resolved. Similar

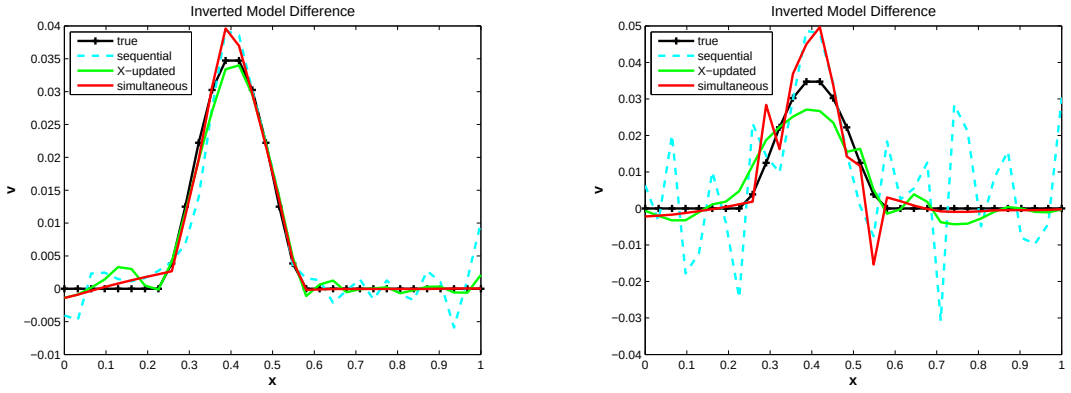

(a) (b)

Figure 5: Inverted model difference: (a) no noise (b) 5% noise and $.5\Delta x$ random receiver mispositioning. Note that the result of simultaneous inversion is closest to zero outside of the area of "production-induced" change. The cross-updating result is a good qualitative approximation to simultaneous inversion. [**CR**]

results have been achieved for multiple alternative noise realizations, with the simultaneous inversion always delivering the best *model difference* result and cross-updating providing a good qualitative approximation.

CONCLUSIONS AND WAY FORWARD

We propose a new technique for time-lapse full waveform inversion that can provide a robust alternative to the existing methods. Applying the method to a one-dimensional test problem achieved a significant reduction of artifacts in the model difference. However, choice of the weighting operator $\mathbf{W}$ is determined by prior knowledge of where production-induced velocity changes are likely to occur. In the absence of such prior knowledge, a frequency-dependent weighting of the model difference regularization term may have to be used to achieve a balance between the accuracy of data fitting and the desired properties of the model difference (Aster et al., 2012). In such a case, our proposed cross-updating method would offer an attractive alternative to the regularized simultaneous inversion as it delivers qualitatively accurate results without the need to specify regularization parameters.

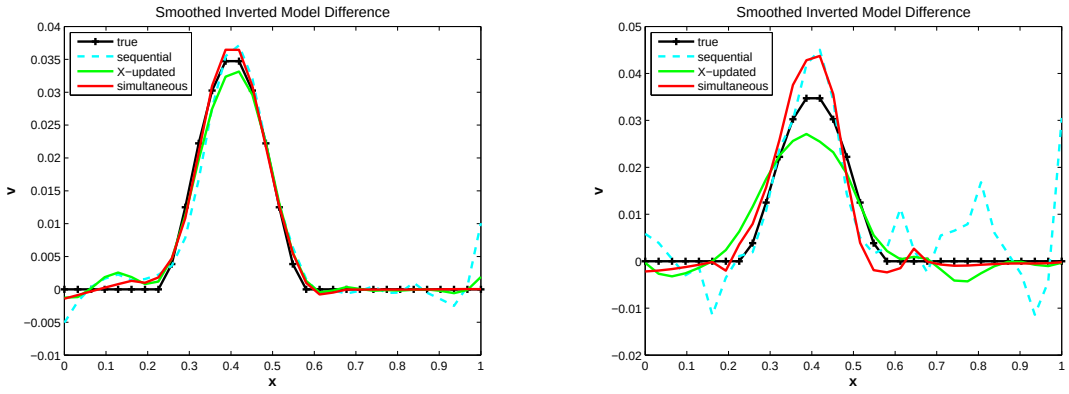

(a) (b)

Figure 6: Smoothed inverted model difference: (a) no noise (b) 5% noise and $.5\Delta x$ random receiver mispositioning. Even after smoothing the simultaneous inversion and its cross-updating approximation are superior to the result of iterated sequential inversion. [**CR**]

The cross-updating technique does not require the development of any new tools and, in principle, can be applied to time-lapse FWI problems of any scale and complexity. The simultaneous inversion based on optimizing the objective function 5-9 can be applied to regularized time-lapse velocity inversion using a prior model difference derived from geomechanical studies (Maharramov, 2012).

We did not apply the regularized simultaneous inversion to the double difference method (i.e., with a nonzero term 6 in the objective function) and this will require further study. In our next work we intend to apply the simultaneous time-lapse FWI and cross-updating methods to field data, and study the feasibility of using geomechanical model-difference priors.

REFERENCES

Asnaashari, A., R. Brossier, S. Garambois, F. Audebert, P. Thore, and J. Virieux, 2012, Time-lapse imaging using regularized FWI: a robustness study: SEG Technical Program Expanded Abstracts, 1–5.

Aster, R. C., B. Borchers, and C. H. Thurber, 2012, Parameter estimation and inverse problems: Elsevier.

Ayeni, G. and B. Biondi, 2012, Time-lapse seismic imaging by linearized joint inversion a valhall field case study: SEG Technical Program Expanded Abstracts, 1–6.

Barkved, O. and T. Kristiansen, 2005, Seismic time-lapse effects and stress changes: Examples from a compacting reservoir: The Leading Edge, **24**, 1244–1248.

Maharramov, M., 2012, Identifying reservoir depletion patterns with applications to seismic imaging: SEP Report 147, 193–218.

Nocedal, J. and S. Wright, 2006, Numerical optimization: Springer.

Plessix, R.-E., S. Michelet, H. Rynja, H. Kuehl, C. Perkins, J. W. de Maag, and P. Hatchell, 2010, Some 3D applications of full waveform inversion in 3D Full Waveform Inversion Workshop – a Game Changing Technique?: 72nd EAGE Conference and Exhibition.

Routh, P., G. Palacharla, I. Chikichev, and S. Lazaratos, 2012, Full wavefield inversion of time-lapse data for improved imaging and reservoir characterization: SEG Technical Program Expanded Abstracts, 1–6.

Virieux, J. and S. Operto, 2009, An overview of full waveform inversion in exploration geophysics: Geophysics, **74**, WCC127–WCC152.

Virieux, J., S. Operto, B. H. Ali, R. Brossier, V. Etienne, F. Sourbier, L. Giraud, and A. Haidar, 2009, Seismic wave modeling for seismic imaging: The Leading Edge - Special Section: Seismic Modeling, 538–544.

Watanabe, T., S. Shimizu, E. Asakawa, and T. Matsuoka, 2004, Differential waveform tomography for time-lapse crosswell seismic data with application to gas hydrate production monitoring: 74th SEG Conference and Exhibition, Expanded Abstracts, 2323–2326.